

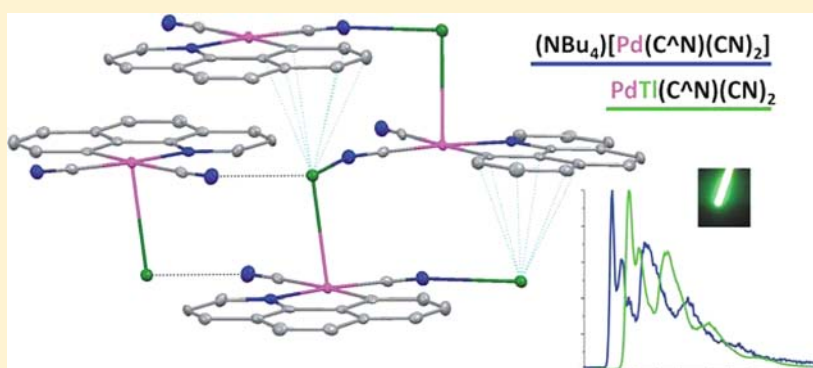
New Dicyano Cyclometalated Compounds Containing Pd(II)–Tl(I) Bonds as Building Blocks in 2D Extended Structures: Synthesis, Structure, and Luminescence Studies

Violeta Sicilia,^{*,†} Juan Forniés,[‡] Sara Fuertes,[‡] and Antonio Martín[‡]

[†]Instituto de Síntesis Química y Catálisis Homogénea (ISQCH), CSIC - Universidad de Zaragoza, Departamento de Química Inorgánica, Escuela de Ingeniería y Arquitectura de Zaragoza, Campus Río Ebro, Edificio Torres Quevedo, 50018 Zaragoza, Spain

[‡]Instituto de Síntesis Química y Catálisis Homogénea (ISQCH), CSIC - Universidad de Zaragoza, Departamento de Química Inorgánica, Facultad de Ciencias, Pedro Cerbuna 12, 50009 Zaragoza, Spain

S Supporting Information



ABSTRACT: New mixed metal complexes $[\text{PdTl}(\text{C}^{\wedge}\text{N})(\text{CN})_2]$ [$\text{C}^{\wedge}\text{N}$ = 7,8-benzoquinolate (bzq, **3**); 2-phenylpyridinate (ppy, **4**)] have been synthesized by reaction of their corresponding precursors $(\text{NBu}_4)[\text{Pd}(\text{C}^{\wedge}\text{N})(\text{CN})_2]$ [$\text{C}^{\wedge}\text{N}$ = bzq (**1**), ppy (**2**)] with TlPF₆. Compounds **3** and **4** were studied by X-ray diffraction, showing the not-so-common Pd^{II}–Tl^I bonds. Both crystal structures exhibit 2-D extended networks fashioned by organometallic “PdTl(C[∧]N)(CN)₂” units, each one containing a donor–acceptor Pd(II)–Tl(I) bond, which are connected through additional Tl⋯N≡C contacts and weak Tl⋯π (bzq) contacts in the case of **3**. Solid state emissions are red-shifted compared with those of the precursors and have been assigned to metal–metal′-to-ligand charge transfer (MM′LCT [$d/s \sigma^*(\text{Pd},\text{Tl}) \rightarrow \pi^*(\text{C}^{\wedge}\text{N})$]) mixed with some intraligand (${}^3\text{IL}[\pi(\text{C}^{\wedge}\text{N}) \rightarrow \pi^*(\text{C}^{\wedge}\text{N})]$) character. In diluted solution either at room temperature or 77 K, the Pd–Tl bond is no longer retained as confirmed by mass spectrometry, NMR, and UV–vis spectroscopic techniques.

INTRODUCTION

Homo- and heteropolynuclear species that have metallophilic interactions between closed- or pseudo-closed-electron-shell atoms and ions (d^8 , d^{10} , or $d^{10} s^2$ systems) have attracted considerable interest owing to their unique chemical bonding, structure, reactivity, and importance in catalytic processes.^{1–7} Metallophilic bonding that involves square-planar platinum(II) complexes acting as a Lewis base has been known for several decades and has led to a large variety of polymeric assemblies, ranging from simple bimetallic compounds to high-nuclearity clusters and extended structures. From a molecular-orbital point of view, in the presence of a strong ligand field, these interactions mainly involve the d_z^2 orbital, which is the highest occupied molecular orbital (HOMO).^{8,9} According to this consideration, square planar d^8 complexes act as two-electron donor metalloligands for Lewis-acidic metals, forming a dative metal–metal bond.

In the chemistry of platinum(II), electron-rich anionic perhalophenyl^{10,11} or alkynyl^{12–20} complexes have been successfully used in the synthesis of cluster complexes containing Pt(II) → M (M = Cu^I, Ag^I, Au^I, Cd^{II}, Hg^{II}, Tl^I, Sn^{II}, or Pb^{II}) donor–acceptor bonds, with the Pt(II) → Ag(I) compounds being the most numerous.^{10,14–16,21–23} Also, platinum(II) complexes containing chromophoric C,N-cyclometalating ligands such as 2-phenylpyridine (Hppy), 2-(2-thienyl)pyridine (Hthpy), or benzo{h}quinoline (Hbzq)²⁴ or C[∧]N[∧]C-cyclometalated ligands have been successfully used for preparing Pt → M derivatives^{21,23,25–30} even when neutral substrates of the type $[\text{Pt}(\text{C}^{\wedge}\text{N})_2]$ and $[\text{Pt}(\text{C}^{\wedge}\text{N})(\text{S}^{\wedge}\text{S})]$ ($\text{C}^{\wedge}\text{N}$ = C,N-cyclometalated ligand; $\text{S}^{\wedge}\text{S}$ = pyrrolidinedithiocarbamate (pdtc), dimethyldithiocarbamate (dmdtc)),^{23,30–32} or the

Received: April 20, 2012

Published: September 21, 2012

Scheme 1

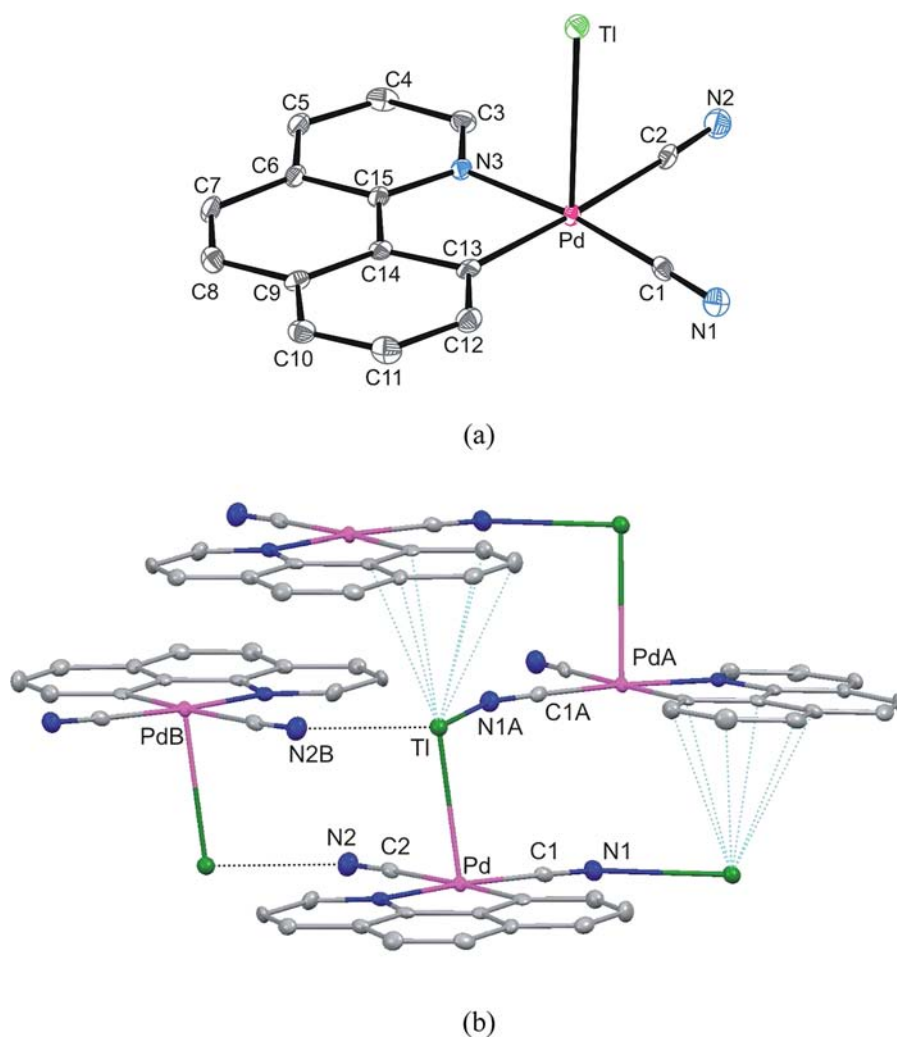
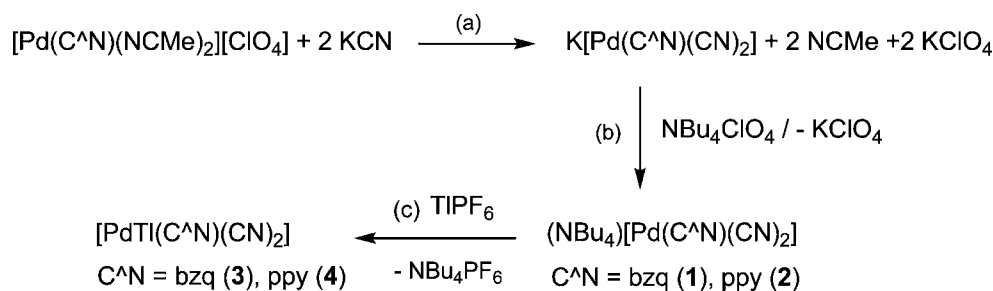


Figure 1. (a) ORTEP view of $[\text{PdTi}(\text{bzq})(\text{CN})_2]$ (3). Ellipsoids are drawn at the 50% probability level. Hydrogen atoms have been omitted for clarity. (b) Supramolecular structure view.

cationic $[\text{Pt}(\text{phpy})_9\text{S3}]^+$ (phpy = 2-phenylpyridine; 9S3 = 1,4,7-trithiacyclononane)²⁸ were used.

Lewis-acidic metal complexation often has a marked effect on the optical properties of organoplatinum compounds. Many of these compounds feature interesting optical properties such as long-lived, low-energy luminescence.^{33–35} Metal–metal-bonded polymeric units often constitute a chromophore by themselves, giving rise to luminescence attributed to metal-to-metal charge transfer (MM'CT) transitions.^{22,36,37} However, the origin of the luminescence in these polymeric compounds sometimes might be different, especially when the platinum

moiety already contains a chromophore group within the molecule.^{13,25,37,38}

Thus, as seen above, a wide variety of organometallic platinum(II) compounds containing dative metal–metal bonds have been prepared with diverse ancillary ligands and acceptor fragments. However, the palladium(II) counterparts are not as likely to form donor–acceptor metal–metal bonds^{39,40} which is mainly due to the relativistic effects. It is well-known that most of the metal–metal bonds involve metal ions from the third row of the transition series, where the relativistic effects are believed to contribute significantly to the bonding.^{24,41–43} To our knowledge, Pd/M compounds with Pd → M dative bonds

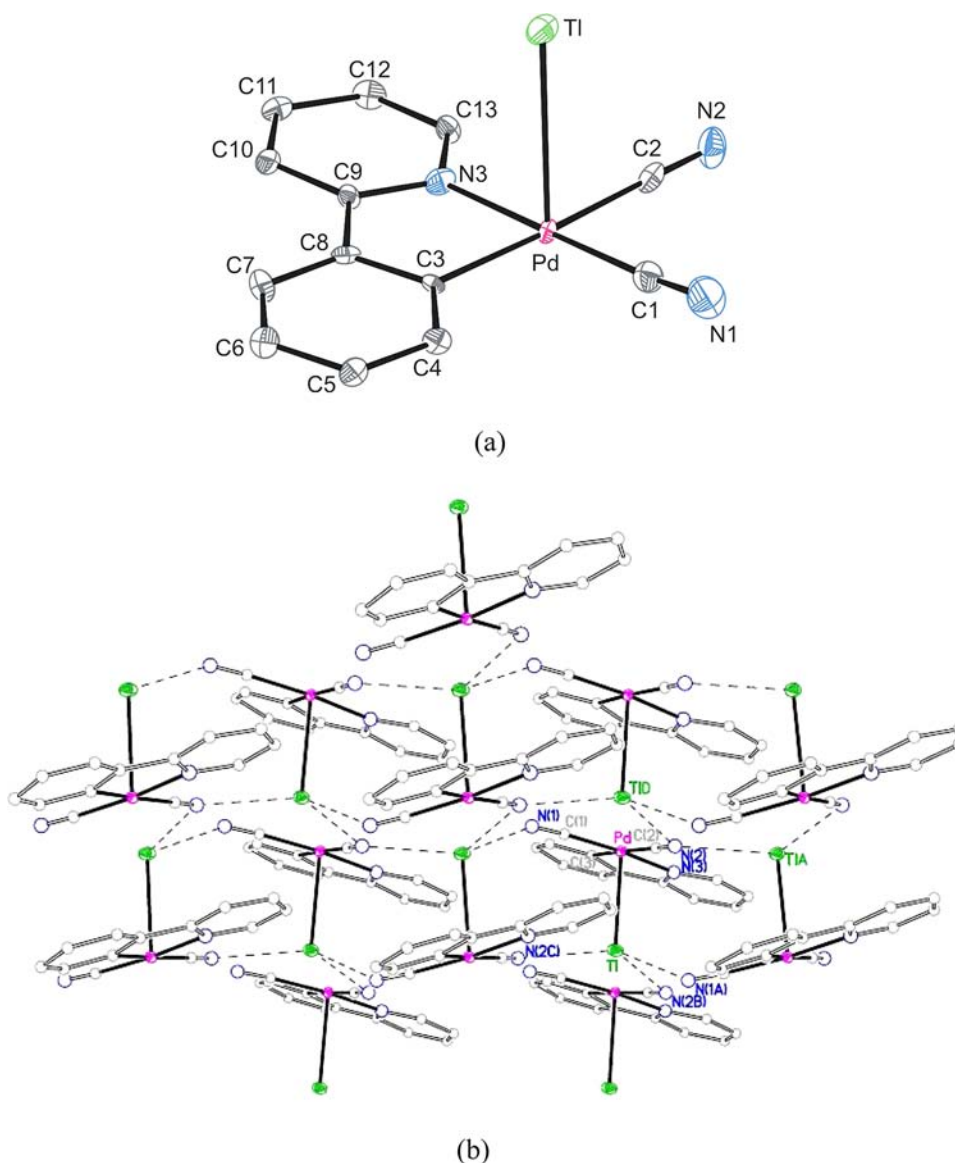


Figure 2. a) ORTEP view of $[\text{PdTl}(\text{ppy})(\text{CN})_2]$ (**4**). Ellipsoids are drawn at the 50% probability level. Hydrogen atoms have been omitted for clarity. (b) Supramolecular structure view.

are very limited in the literature,^{44–56} and only a few of them display analogous crystal structures to their corresponding platinum derivatives.^{49,52,53,55} In particular when the metal–metal bond involves Pd^{II} and Tl^{I} ions, the number of reported structures decreases considerably: two palladium selenide salts, $\text{Tl}_2\text{Pd}_4\text{Se}_6$ ($\text{Pd}-\text{Tl} = 2.941 \text{ \AA}$)⁵⁴ and Tl_2PdSe_2 ($\text{Pd}-\text{Tl} = 2.923 \text{ \AA}$);⁵⁶ two cyanide compounds $[\text{Tl}(\text{crown-P}_2)\text{Pd}(\text{CN})_2](\text{PF}_6)$ ($\text{Pd}-\text{Tl} = 2.897 \text{ \AA}$)⁵⁵ and $\text{Tl}_2\text{Pd}(\text{CN})_4$ (3.173 \AA);⁵² the sandwich-type $[\{(\text{Bu}_2\text{bpy})\text{PdMe}_2\}_3\text{Tl}_2](\text{PF}_6)_2$ ($\text{Pd}-\text{Tl} = 2.793\text{--}2.994 \text{ \AA}$),⁴⁸ and merely one structure within the electronic configuration $4d^8\text{--}5d^{10}$ ($\text{Pd}^{\text{II}}\text{--}\text{Tl}^{\text{III}}$), $[\text{Pd}(\mu\text{-O}_2\text{CMe})_4\text{Tl}(\text{O}_2\text{CMe})]$.⁵⁵

In this work, we describe two new Pd/Tl metal mixed complexes whose crystal structures and optical properties are significantly related to those found in the analogous Pt/Tl derivatives previously prepared in our group. They were synthesized by reacting TlPF_6 with the cyanide complexes $(\text{NBu}_4)[\text{Pd}(\text{C}^{\wedge}\text{N})(\text{CN})_2]$ [$\text{C}^{\wedge}\text{N} = \text{bzq}$ (**1**), ppy (**2**)]. As a result, extended structures containing Pd(II)–Tl(I) metal-philic interactions have been observed. Their photophysical

properties are also discussed and compared with those of their starting materials (**1**, **2**) and also with the analogous Pt(II)/Tl(I) derivatives.

RESULTS AND DISCUSSION

Synthesis and Characterization of the Pd(II) Cyanide Compounds $\text{NBu}_4[\text{Pd}(\text{C}^{\wedge}\text{N})(\text{CN})_2]$ [$\text{C}^{\wedge}\text{N} = \text{bzq}$ (1**), ppy (**2**)].** Compounds $\text{NBu}_4[\text{Pd}(\text{C}^{\wedge}\text{N})(\text{CN})_2]$ [$\text{C}^{\wedge}\text{N} = \text{bzq}$ (**1**), ppy (**2**)] were prepared by addition of KCN to a suspension of the corresponding compound $[\text{Pd}(\text{C}^{\wedge}\text{N})(\text{NCMe})_2]\text{ClO}_4$ [$\text{C}^{\wedge}\text{N} = \text{bzq}$ (**A**), ppy (**B**)] in 2:1 molar ratio in methanol and the subsequent addition of the equimolar amount of NBu_4ClO_4 to the “in situ” freshly prepared solution of $\text{K}[\text{Pd}(\text{C}^{\wedge}\text{N})(\text{CN})_2]$ (see Scheme 1, steps a and b, and Experimental Section).

Compounds **1** and **2** were isolated as white, air-stable solids in high yields and fully characterized (see Experimental Section). The cis arrangement of the two terminal CN^- ligands in compounds **1** and **2** is evident in their IR spectra^{57,58} and in the ^{13}C NMR spectra of compounds $(\text{NBu}_4)[\text{Pd}(\text{C}^{\wedge}\text{N})(\text{CN})_2]$ [$\text{C}^{\wedge}\text{N} = \text{bzq}$ (**1'**), ppy (**2'**)] that were prepared in the

same way as that for **1** and **2**. Two ν_{CN} absorptions around 2110 and 2120 cm^{-1} were observed in the IR spectra of **1** and **2**.

Two doublets at ca. 145 and 131 ppm were observed in the ^{13}C NMR spectra of **1'** and **2'** corresponding to the $^{13}\text{CN}^-$ groups *trans* to $\text{C}^{\wedge}\text{N}$ and $\text{N}^{\wedge}\text{C}$, respectively, by resemblance with their analogous Pt derivatives.⁵⁹ Compounds **1** and **2** were used as starting materials in the synthesis of the Pd–Tl clusters as described.

Synthesis and Characterization of Pd–Tl Clusters.

Treatment of compounds $[\text{NBu}_4][\text{Pd}(\text{C}^{\wedge}\text{N})(\text{CN})_2]$ [$\text{C}^{\wedge}\text{N} = \text{bzq}$ (**1**), *ppy* (**2**)] with the equimolar amount of TlPF_6 in methanol solution causes the precipitation of $[\text{PdTl}(\text{C}^{\wedge}\text{N})(\text{CN})_2]$ [$\text{C}^{\wedge}\text{N} = \text{bzq}$ (**3**), *ppy* (**4**)] as pale yellow solids, which were washed with dichloromethane and obtained as analytically pure solids in good yield (See Experimental Section and Scheme 1, step c). The most significant feature of the IR spectra is the presence of two $\nu_{\text{C}\equiv\text{N}}$ (2132, 2112 cm^{-1} **3**; 2118, 2107 cm^{-1} **4**) absorptions according to the *cis* arrangement of the cyanide ligands.³⁷ The small shift of these absorptions in relation to those in the corresponding starting complexes [$\nu_{\text{C}\equiv\text{N}} = 2121, 2111 \text{ cm}^{-1}$ **1**; 2122, 2113 cm^{-1} **2**] is in agreement with the weak interaction between these groups and the thallium center as observed in their X-ray structures described below.

Crystal structures of compounds **3** and **4** appear in Figures 1 and 2, and selected bond distances and angles are listed in Table 1. As can be seen, these compounds generate extended networks formed by organometallic “ $\text{PdTl}(\text{C}^{\wedge}\text{N})(\text{CN})_2$ ” units, each one containing a donor–acceptor Pd(II)–Tl(I) bond, which are connected through additional $\text{Tl}\cdots\text{N}\equiv\text{C}$ contacts. The molecular structures reveal a square pyramidal environment around the palladium center with the thallium atom being located in the apical position. The Pd–Tl bond distance [**3**, 3.0210(3) Å; **4**, 3.0425(7) Å] and the angle of the Pd–Tl vector with the normal to the palladium coordination plane [**3**, 8.4(1)° (**3**) and 10.3(2)° (**4**)] are comparable to those reported in related systems containing donor–acceptor M(II)–Tl(I) (M = Pd,^{48,52,54–56} Pt²⁵) bonds.

The Pd–Tl bond distances in **3** and **4** are only slightly longer than those seen in their analogous Pt(II) complexes $[\text{PtTl}(\text{C}^{\wedge}\text{N})(\text{CN})_2]$ ($\text{C}^{\wedge}\text{N} = \text{bzq}$, 2.9910(7) Å; *ppy*, 3.0085(10) Å)²⁵ in agreement with the lanthanide contraction that affects the third row transition metals.^{42,52,60} The base of the pyramid containing the Pd center and the four atoms bonded to it is planar; the narrow bite angle in the metallocycle [$\text{C}–\text{Pd}–\text{N} = 82.03(15)^\circ$ (**3**); $81.1(3)^\circ$ (**4**)] and the Pd– $\text{N}^{\wedge}\text{C}$, Pd– $\text{C}^{\wedge}\text{N}$, and Pd– $\text{C}\equiv\text{N}$ bond distances are all in the range of those observed in palladium complexes with $\text{C}^{\wedge}\text{N}$ -cyclometalated^{161,62} and cyanide^{55,63,64} ligands. The extended lattices show the Tl center of each “ $\text{PdTl}(\text{C}^{\wedge}\text{N})(\text{C}\equiv\text{N})_2$ ” unit to be connected to two (in compound **3**) or three (in compound **4**) nitrogen atoms of CN^- ligands belonging to neighboring units generating 2-D structures. As a result, in compound **4**, the thallium centers exhibit a distorted tetrahedral environment, while in **3** the local geometry around the thallium centers suggests a strong stereochemical demand of the electron lone pair,⁶⁵ being similar to that observed in $[\text{PtTl}(\text{bzq})(\text{CN})_2]$ ²⁵ or in the yellow polymorph of $[\text{Tl}\{\text{Pt}(\text{C}_4\text{H}_9\text{N}_4)(\text{CN})_2\}]$.⁶⁶ The observed $\text{Tl}\cdots\text{N}(\text{CN})$ contacts [2.626(3)–2.837(11) Å] are longer than expected for a covalent bond $\text{Tl}–\text{N}$ ⁶⁷ but comparable to those found in related derivatives containing cyanide groups such as $[\text{Tl}_2\text{Pt}(\text{CN})_4]$ (2.80–3.04 Å),⁶⁸

Table 1. Selected Bond Lengths (Å) and Angles (deg) for Compounds **3** and **4**

	3 ^a	4 ^b
Pd–Tl	3.0210(3)	3.0425(7)
Pd–C(1)	1.951(4)	2.030(11)
Pd–C(2)	2.056(4)	2.004(10)
Pd–C(3)		2.068(8)
Pd–C(13)	2.025(4)	
Pd–N(3)	2.076(3)	2.039(8)
Tl–N(1A)	2.626(3)	2.837(11)
Tl–N(2B)	2.721(4)	2.759(9)
Tl–N(2C)		2.956(9)
N(1)–C(1)	1.152(5)	1.147(15)
N(2)–C(2)	1.149(6)	1.132(13)
C(1)–Pd–C(2)	94.42(15)	88.9(4)
C(1)–Pd–C(3)		95.6(4)
C(1)–Pd–C(13)	90.26(17)	
C(2)–Pd–N(3)	93.27(14)	94.5(4)
C(3)–Pd–N(3)		81.1(3)
C(13)–Pd–N(3)	82.03(15)	
C(1)–Pd–Tl	94.54(11)	94.5(3)
C(2)–Pd–Tl	82.54(11)	82.7(3)
C(3)–Pd–Tl		97.3(2)
C(13)–Pd–Tl	97.66(11)	
N(3)–Pd–Tl	88.08(9)	82.4(2)
N(2B)–Tl–N(1A)	102.80(11)	81.0(3)
N(2B)–Tl–Pd	96.02(8)	106.9(2)
N(1A)–Tl–Pd	92.09(7)	111.9(2)
C(1A)–N(1A)–Tl	148.0(3)	149.8(9)
C(2B)–N(2B)–Tl	142.7(3)	110.5(7)
C(2C)–N(2C)–Tl		124.4(7)
N(1)–C(1)–Pd	178.5(4)	176.2(9)
N(2)–C(2)–Pd	175.9(3)	177.7(8)

^aSymmetry elements used to generate equivalent atoms for **3**: A, 0.5 – x, y, z – 0.5; B, –x, 1 – y, –1 – z; C, 0.5 + x, 1 – y, –1.5 – z; D, 1 – x, 1 – y, –2 – z; E, 0.5 – x, y, 0.5 – z. ^bSymmetry elements used to generate equivalent atoms for **4**: A, 1 + x, y, z; B, –1 + x, y, z; C, –1 – x, 0.5 + y, 0.5 – z; D, –1 – x, –0.5 – y, 0.5 – z.

$[\text{Tl}_2\text{Pd}(\text{CN})_4]$ (2.85–3.06 Å),⁵² both the red and yellow polymorphs of $[\text{Tl}\{\text{Pt}(\text{C}_4\text{H}_9\text{N}_4)(\text{CN})_2\}]$ (2.691(9), 2.687(7) Å),⁶⁶ and $[\text{trans,trans,trans-Tl}_2\{\text{Pt}(\text{C}_6\text{F}_5)_2(\text{CN})_2\}(\text{CH}_3\text{COCH}_3)_2]_n\{\text{Tl}\{\text{Tl}\{\text{cis-Pt}(\text{C}_6\text{F}_5)_2(\text{CN})_2\}(\text{H}_2\text{O})\}_n\}$.³⁶ As can be seen in Figures 1 and 2, the CN^- ligands display a bent $\mu^2\text{-}\kappa\text{C}:\kappa\text{N}$ bridging mode in compound **3**, while in **4** either $\mu_2\text{-}\kappa\text{C}:\kappa\text{N}$ and $\mu_3\text{-}\kappa\text{C}:\kappa\text{N}:\kappa\text{N}$ bridging modes are present. As was observed in $[\text{PtTl}(\text{C}^{\wedge}\text{N})(\text{CN})_2]$ ($\text{C}^{\wedge}\text{N} = \text{bzq}$, *ppy*),²⁵ the Tl–N–C angles are close to 145° for a $\mu^2\text{-}\kappa\text{C}:\kappa\text{N}$ coordination mode and smaller (110°–125°) for a $\mu_3\text{-}\kappa\text{C}:\kappa\text{N}:\kappa\text{N}$ one.

A perspective view of the crystal structure in compound **3** (Figure 1b) reveals that between two “ $\text{PdTl}(\text{bzq})(\text{CN})_2$ ” units of adjacent layers, there are two Tl–CN–Pd bridges to give eight-membered cycles (black dashed line). Weak interactions of each Tl center with the π electron density of a ring of an adjacent benzoquinolate group are also observed; the $\text{Tl}\cdots\pi(\text{arene})$ separations, ca. 3.45 Å (cyan dashed line), are quite similar to those observed in $[\text{PtTl}(\text{bzq})(\text{C}\equiv\text{C}-\text{C}_3\text{H}_4\text{N}-2)]\cdot\text{CH}_2\text{Cl}_2$.²⁵ According to this, in both crystal structures, the thallium center exhibits three additional interactions apart from the Pd–Tl metal–metal bond. Whereas in compound **3** the thallium is interacting with the π electron density of a benzoquinolate group and two cyanides, in **4**, the thallium

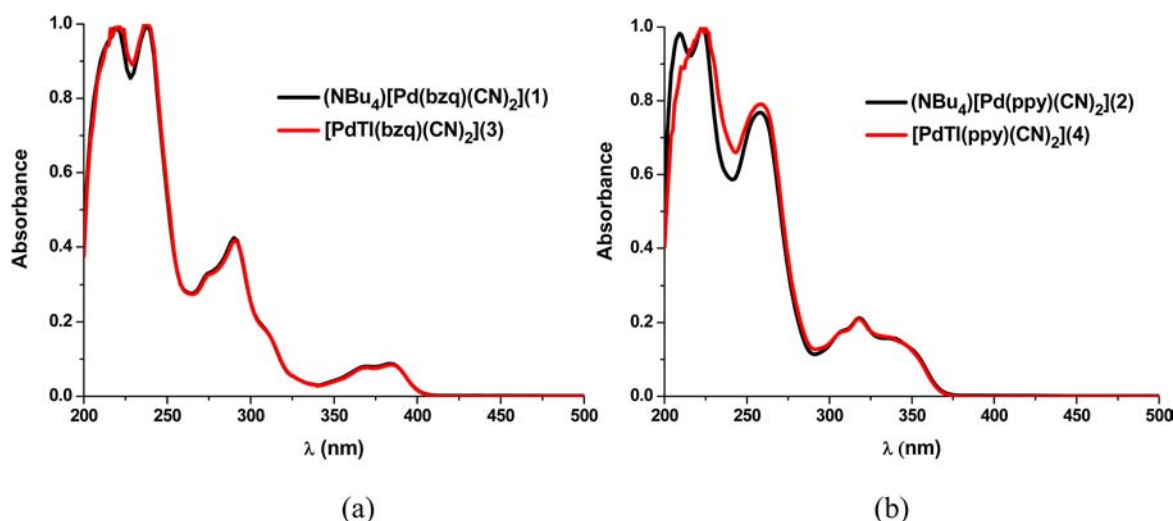


Figure 3. Normalized UV–visible absorption spectra of **1** and **3** (a) and **2** and **4** (b) in methanol (10^{-4} M) at 298 K.

is interacting with three different cyanide ligands. Also, in both cases the relatively long interlayer separation leads to C–C distances between adjacent C[^]N groups that are longer than 3.8 Å, indicating the absence of π – π interactions in these complexes.

Compounds **3** and **4** crystallize in the same space groups (*Pccn*, **3**; *P2₁2₁2₁*, **4**) as the corresponding Pt/Tl derivatives,²⁵ and therefore, as discussed above, their crystal structures are essentially identical too. Additionally, the Pd derivatives were prepared in the same way as the Pt ones, and the metal center exhibits the same coordination environment (the same ligands, coordination number, and geometry). Taking all this into consideration, these compounds meet all criteria on which to base the direct comparison of the relative sizes of palladium(II) and platinum(II).^{69–71} For this comparison, we have focused on the bzq derivatives [PtTl(bzq)(CN)₂]²⁵ and [PdTl(bzq)(CN)₂] (**3**) for which the bond distances have lower standard deviations than those of the ppy complexes. So, the average Pt–C_{CN} distance [1.9775 Å] in [PtTl(bzq)(CN)₂] is smaller than the average Pd–C_{CN} distance [2.0035 Å] in [PdTl(bzq)(CN)₂]. Assuming that the covalent radius of C(sp) is the same in both complexes and a value of $r(\text{C}(\text{sp})) = 0.60$ Å, the covalent radius of five-coordinated platinum(II) [1.3775 Å] is found to be ca. 2% smaller than the covalent radius of five-coordinated palladium(II) [1.4035 Å]. This result agrees well with the elongation of the Pd–Tl bond distance (3.0210 Å, **3**) with respect to the Pt–Tl one (2.9910 Å) in [PtTl(bzq)(CN)₂], and this is also in line with the deductions made by Schmidbaur et al. for the gold and silver covalent radii. For complexes **3** and **4**, conductivity measurements in methanol solutions (49.74 **3**; 52.40 Ω^{-1} cm² mol⁻¹ **4**), mass spectra (m/z [Pd(bzq)(CN)₂]⁻ 336, 100%, **3**; [Pd(pppy)(CN)₂]⁻ 312, 100%, **4**), and ¹H NMR signals are almost equal to those of the precursors (**1** and **2**), which suggest the dissociation of the Pd–Tl bimetallic unit in solution.

Photophysical Properties. The UV–vis absorption spectra of compounds **1–4** in methanol solutions are represented in Figure 3 and the corresponding data are summarized in Table 2. The absorption bands observed for (NBu₄)[Pd(C[^]N)(CN)₂] [C[^]N = bzq (**1**), ppy (**2**)] are similar in profile but blue-shifted with respect to those of the corresponding platinum compounds (Figure S1, Supporting Information).⁷²

Table 2. Absorption Data for Compounds **1–4** in 10^{-4} M Solutions at 298 K

compd	solvent	λ_{abs} , nm ($\epsilon \times 10^3$, M ⁻¹ cm ⁻¹)
1	CH ₂ Cl ₂	242 (40.5), 278 (14.9), 292 (18.1), 310sh (8.5), 347sh (2.2), 370 (3.4), 386 (4)
	MeOH	220 (39.1), 238 (39.6), 274 (12.9), 290 (16.8), 308sh (7.3), 347sh (2.2), 370 (3.2), 384 (3.5)
	MeCN	218 (41.3), 240 (40.7), 278 (15.2), 291 (17.8), 310sh (7.9), 348sh (1.7), 368 (3.2), 384 (3.7)
2	CH ₂ Cl ₂	231 (32.1), 263 (31.7), 308sh (7.4), 319 (8.7), 341 (6.6), 353sh (5.2)
	MeOH	209 (29.6), 229 (37), 258 (29.4), 307sh (6.7), 318 (8.1), 340 (4.7), 349sh (3.8)
	MeCN	210 (39.4), 225 (39.9), 260 (33.4), 308sh (7.7), 317 (8.9), 338 (6.9), 349sh (5.5)
3	MeOH	220 (38.2), 237 (38.6), 275sh (12.5), 291 (16.1), 309sh (6.8), 350sh (1.5), 369 (3), 384 (3.3)
4	MeOH	223 (38.8), 258 (30.7), 308sh (6.8), 318 (8.1), 345 (5.6), tail to 370

Previous TD-DFT calculations on the platinum complexes [Pt(C[^]N)(CN)₂]⁻ showed unambiguously that the lowest energy absorption corresponds mainly to LC [$\pi(\text{C}^{\wedge}\text{N}) \rightarrow \pi^*(\text{C}^{\wedge}\text{N})$] transitions mixed with some MLCT character.⁵⁷ By analogy, in complexes **1** and **2**, the lowest energy absorptions can be tentatively assigned to the same kind of transitions. As more extensive aromaticity in the bzq ligand with respect to ppy lowers the π^* energy level, a red shift is observed for the lower energy LC/MLCT transition of complex **1** (C[^]N = bzq) with respect to that of **2** (C[^]N = ppy).⁷³ The partial ¹MLCT character of these low-energy transitions is consistent with their blue shift vs the corresponding platinum complexes (NBu₄)[Pt(C[^]N)(CN)₂].

As can be seen in Figure 3 and Table 2, the UV–vis spectra of the mixed Pd/Tl complexes [PdTl(C[^]N)(CN)₂] (C[^]N = bzq (**3**), ppy (**4**)) exhibit identical features to their corresponding precursors, **1** and **2**. This fact is consistent with the rupture of the Pd–Tl bonds in solution, as indicated by other analytical data mentioned previously. Therefore, the low-energy absorption bands in compounds **1–4** are attributed to ¹LC transitions with some ¹MLCT contribution in the anionic [Pd(C[^]N)(CN)₂]⁻ fragments. In the solid state, the diffuse reflectance UV–vis spectra of powder samples of complexes **1–4** appear red-shifted compared with those in

solutions of methanol (see Figure S2, Supporting Information). No significant differences are observed among the solid spectra of the mixed Pd/Tl complexes with respect to those of their corresponding precursors **1** and **2**. It suggests that the Pd–Tl bonds existing in the solid state do not have any apparent effect in the absorption bands of these heteronuclear complexes.

Compounds **1**–**4** are luminescent only at 77 K both in the solid state and in methanol (10^{-4} M) glassy solutions (Table 3,

Table 3. Emission Data for Complexes 1–4 at 77 K

compd	state	λ_{exc} nm	λ_{em} nm	τ , μs
1	solid	(365–405)	479 max, 489, 514, 557 ^a	6889 (479)
	CH ₂ Cl ₂ ^c	370, 385	477 max, 485 sh, 513, 553 ^a	
	MeOH ^c	365, 385	472 max, 480 sh, 508, 546 ^a	
2	solid	370	469 max, 476 sh, 485, 493, 504, 522, 535, 546 ^b	356 (469)
	CH ₂ Cl ₂ ^c	320–360	464, 479, 488 sh, 498, 526, 538 ^a	
	MeOH ^c	320–360	462, 478 sh, 486 sh, 497, 523, 533 ^a	
3	solid	430	496 max, 506, 536, 579 ^b	1441 (496)
	MeOH ^c	350, 370, 385	472 max, 480 sh, 506, 546 ^a	
4	solid	420	508, 545 max, 585 sh ^b	211 (508)
	MeOH ^c	320–360	462, 486 sh, 496, 524, 534 ^a	

^aTail to 650 nm. ^bTail to 700 nm. ^c 10^{-4} M.

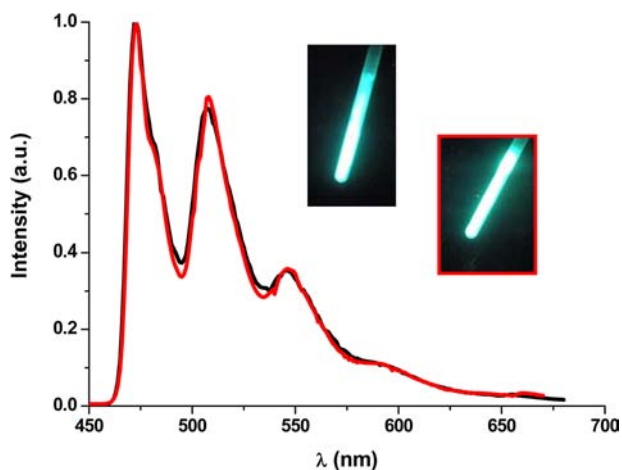


Figure 4. Normalized emission spectra of **1** (black) and **3** (red) in methanol (10^{-4} M) at 77 K. Pictures of **1** and **3** were taken with a UV lamp at $\lambda_{\text{ex}} = 365$ nm.

Figures 4 and 5 and Figures S3–S9, Supporting Information), which is usual in palladium complexes because of the presence of low-lying metal-centered (MC) excited states;⁷⁴ this phenomenon occurs despite the strong field ligands (bzq, ppy, and cyanide) existing in these complexes. The palladium compounds **1** and **2** in the solid state and in a rigid matrix of methanol (Figures S3 and S4, Supporting Information, and Table 3) show a bluish structured emission (λ_{max} ca. 470 nm) with vibronic spacing (1370 – 1501 cm^{-1}) typical of the cyclometalated fragments (bzq or ppy) and lifetimes (6889 μs (**1**, bzq); 356 μs (**2**, ppy)) that are significantly longer than those of their analogous platinum complexes (173 μs (bzq); 23

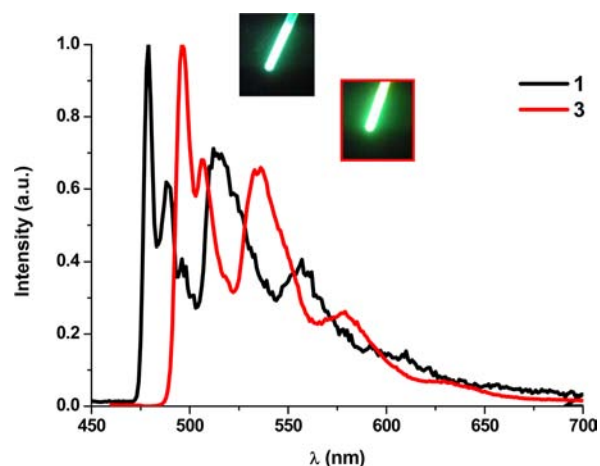


Figure 5. Normalized emission spectra of **1** and **3** in solid state at 77 K. Pictures of **1** (black) and **3** (red) taken with a UV lamp at $\lambda_{\text{ex}} = 365$ nm.

μs (ppy)).^{57,58} This emission has been attributed tentatively to a ³IL emissive state with little if any ³MLCT contribution. The small MLCT contribution could be supported by the rather small solvatochromic effect observed in the glassy solution emissions (see Table 3). Emission spectra of the Pd/Tl compounds **3** and **4** in rigid frozen matrix of methanol (10^{-4} and 10^{-5} M, Table 3) are identical and equally structured to those of their precursors **1** and **2** (See Figure 4 for **1** and **3**) showing similar vibronic spacings (ca. 1400 cm^{-1}). This indicates that in frozen diluted methanol solutions of the heteronuclear complexes, the Pd–Tl bonds seem to be broken. Consequently, the photoluminescence of **3** and **4** in glassy frozen diluted solution is also attributed to the same metal-perturbed ³IL emissive state as in their precursors **1** and **2**.

Only in concentrated (10^{-3} M) frozen solutions the emissions depend on the excitation wavelength (see Figures S5 and S6, Supporting Information). Upon excitation at $\lambda \approx 360$ nm, we observe the same emissions as in diluted samples. While, upon excitation at $\lambda > 400$ nm, a less intense new band appears at lower energy (λ (nm) = 500, 534 (max), **3**; 533 (max), **4**).

In the solid state, complex [PdTl(bzq)(CN)₂] (**3**) shows a greenish structured band with vibronic separations of 1106 – 1504 cm^{-1} similar to that observed in the starting compound **1** (Figure 5), yet significantly red-shifted in relation to that. The difference between both maxima is 715 cm^{-1} ($\lambda_{\text{max}} = 496$ nm in **3**; $\lambda_{\text{max}} = 479$ nm in **1**). A same behavior was observed previously for [PtTl(bzq)(CN)₂] in relation to (NBu₄)[Pt-(C[^]N)(CN)₂] ($\Delta \approx 920$ cm^{-1}),²⁵ which was attributed to the raised energy of the HOMO due to the presence of the Pt–Tl bonds. Therefore, this emission is tentatively attributed to a metal–metal'-to-ligand charge transfer, ³MM'LCT [d/s σ^* -(Pd,Tl) $\rightarrow \pi^*$ (C[^]N)], mixed with some intraligand, ³IL [π (C[^]N) $\rightarrow \pi^*$ (C[^]N)], character.

According to this, compound **3** with a Pd–Tl bond distance of $3.0210(3)$ Å exhibits a red shift ($\Delta \approx 715$ cm^{-1}) in relation to its precursor, **1**, smaller than that found for [PtTl(bzq)-(CN)₂] ($\Delta \approx 920$ cm^{-1}), which shows a shorter Pt–Tl bond distance ($2.9910(7)$ Å).²⁵ The solid-state emission of **4** also experiences a significant bathochromic shift compared with its precursor derivative, **2** (Table 3 and Figure S7, Supporting Information). Therefore, solid state emission bands of the Pd(II) \rightarrow Tl(I) compounds (**3** and **4**) are red-shifted and their

lifetimes are reduced (Table 3) compared with those of their corresponding precursors, **1** and **2**.

CONCLUSIONS

The new compounds $(\text{NBu}_4)[\text{Pd}(\text{C}^{\wedge}\text{N})(\text{CN})_2]$ [$\text{C}^{\wedge}\text{N} = \text{bzq}$ (**1**), ppy (**2**)] and $[\text{PdTl}(\text{C}^{\wedge}\text{N})(\text{CN})_2]$ ($\text{C}^{\wedge}\text{N} = \text{bzq}$ (**3**), ppy (**4**)) have been prepared and their photophysical properties investigated. The X-ray diffraction studies on **3** and **4** confirm the formation of the so scarce $\text{Pd}^{\text{II}}-\text{Tl}^{\text{I}}$ dative bonds with $\text{Pd}-\text{Tl}$ distances barely longer than those observed in their analogous $\text{Pt}(\text{II})/\text{Tl}(\text{I})$ compounds. These compounds generate extended networks formed by organometallic “ $\text{PdTl}(\text{C}^{\wedge}\text{N})(\text{CN})_2$ ” units, each one containing a donor–acceptor $\text{Pd}(\text{II})-\text{Tl}(\text{I})$ bond, and are also connected through $\text{Tl}\cdots\text{N}\equiv\text{C}$ contacts. Additionally, the crystal structure of **3** reveals weak $\text{Tl}\cdots\pi$ (arene) contacts of each Tl center with the π electronic density of the phenyl ring from an adjacent benzoquinolate group.

^1H NMR, UV–vis and emission spectroscopy, and mass spectrometry confirm that the $\text{Pd}-\text{Tl}$ bond breaks down in diluted solution either at room temperature or 77 K. It also can be concluded that the emissive properties of **3** and **4** in glassy solutions are clearly dominated by the electronic features of the corresponding organometallic anion $[\text{Pd}(\text{C}^{\wedge}\text{N})(\text{CN})_2]^-$. However, in the solid state, emissions of **3** and **4** are altered by the $\text{Pd}-\text{Tl}$ interactions. Both emission bands display a marked bathochromic shift and shorter lifetimes compared with those of the starting complexes (**1** and **2**) similarly to that observed in the analogous Pt/Tl complexes.

It is worth mentioning the significant relevance of these Pd/Tl complexes, which display identical crystal structures and similar photophysical behavior to those of the corresponding Pt/Tl derivatives. This allowed us to estimate that the covalent radius of $\text{Pd}(\text{II})$ is ca. 2% larger than that of $\text{Pt}(\text{II})$ in a five-coordinated square pyramidal environment. Also this would support the strategy proposed for the Pt/Tl complexes that suggested a different approach to modify the photoluminescence of cyclometalated complexes by tuning the strength of the metal–metal ($\text{M}-\text{M}'$) bonding.

EXPERIMENTAL SECTION

General Procedures and Materials. Elemental analyses were carried out in a Perkin-Elmer 240-B microanalyzer. IR spectra were recorded on a Perkin-Elmer 599 spectrophotometer (Nujol mulls between polyethylene plates in the range 350–4000 cm^{-1}). ^1H NMR spectra were recorded on Varian Unity-300 and Bruker-400 spectrometers, using tetramethylsilane ($\text{Si}(\text{CH}_3)_4$) as standard reference. Numerical schemes for NMR purposes are depicted in Chart 1. Coupling constant, J , is given in hertz (Hz). Mass spectral analyses were performed with a VG AustoSpec instrument. Conductivity measurements were performed in methanol solutions (5×10^{-4} M) with a Philips PW 9509 conductimeter. UV–visible

spectra were obtained on a Unicam UV4 spectrophotometer. For diffuse-reflectance UV measurements, the spectrophotometer was equipped with a Spectralon RSA-UC-40 Labsphere integrating sphere. Emission and excitation spectra were obtained on a Fluorolog FL-3-11 spectrofluorometer using band pathways of 2 nm for both excitation and emission. The steady-state experiments at 77 K were performed using the Fluorolog accessory a “Liquid-nitrogen Dewar flask FL-1013”. The sample is placed in a quartz tube, and immersed in the liquid-nitrogen-filled Dewar. Lifetime measurements were performed with a Fluoromax phosphorimeter, using a nitrogen cryostat with integrated reservoir, Oxford OptistatDN2, which is connected to a temperature controller (Oxford ITC 503S). The lifetime data were fitted using the Origin Pro 7 program.

KCN, K^{13}CN , and TlPF_6 were purchased from commercial sources; $[\text{Pd}(\text{C}^{\wedge}\text{N})(\text{NCMe})_2]\text{ClO}_4^{75}$ were prepared as described elsewhere.

Synthesis of $(\text{NBu}_4)[\text{Pd}(\text{bzq})(\text{CN})_2]$ (1**).** KCN (223.6 mg, 3.434 mmol) was added to a stirred suspension of $[\text{Pd}(\text{bzq})(\text{NCMe})_2]\text{ClO}_4$ (800.7 mg, 1.717 mmol) in MeOH (60 mL). After 1 h at r.t., the mixture was filtered through Celite, and the resulting solution was evaporated to dryness. NBu_4ClO_4 (587.0 mg, 1.716 mmol) and acetone (60 mL) were added to the residue. After stirring for 1 h, the suspension was filtered through Celite, the solution was evaporated to dryness, and the residue was treated with H_2O (3×40 mL). The remaining solid was filtered, dried (110 °C), and recrystallized from $\text{CH}_2\text{Cl}_2/\text{Et}_2\text{O}$ to give pure **1** as a white solid. Yield: 959.6 mg, 97%. Found: C, 63.90; H, 7.34; N, 9.53. Calcd (%) for $\text{C}_{31}\text{H}_{44}\text{N}_4\text{Pd}$: C, 64.29; H, 7.66; N, 9.67. $\nu_{\text{max}}/\text{cm}^{-1}$ 2121s, 2111s ($\text{C}\equiv\text{N}$). δ_{H} (300 MHz, CD_3COCD_3 , 293 K): 9.43 (1H, dd, $J_{2,3} = 5.1$, $J_{2,4} = 1.5$, 2-H), 8.53 (1H, dd, $J_{4,3} = 5.1$, $J_{4,2} = 1.5$, 4-H), 8.27 (1H, d, $J_{9,8} = 7.0$, 9-H), 7.82 (1H, d, $J_{5,6} = 8.6$, 5-H), 7.71 (1H, d, $J_{5,6} = 8.6$, 6-H), 7.69 (1H, dd, $J_{3,4} = 8.1$, $J_{3,2} = 5.1$, 3-H), 7.6 (1H, d, $J_{7-8} = 7.0$, 7-H), 7.45 (1H, t, $J_{8-7} = J_{8-9} = 7.0$, 8-H), 3.46 (8H, m, CH_2 , NBu_4^+), 1.82 (8H, m, CH_2 , NBu_4^+), 1.42 (8H, m, CH_2 , NBu_4^+), 0.95 (12H, t, $^3J_{\text{H-H}} = 7.3$, CH_3 , NBu_4^+). m/z (FAB $^-$) 336 ($[\text{Pd}(\text{bzq})(\text{C}\equiv\text{N})_2]^-$, 100%); Λ_{M} 37.1 $\Omega^{-1}\text{cm}^2\text{mol}^{-1}$, solution 5×10^{-4} M in methanol.

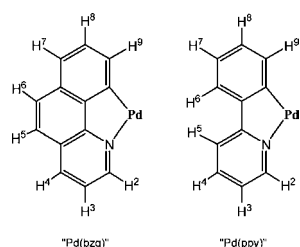
$(\text{NBu}_4)[\text{Pd}(\text{bzq})(^{13}\text{CN})_2]$ (**1'**) was prepared following the method described for **1**, but using K^{13}CN . $\nu_{\text{max}}/\text{cm}^{-1}$ 2074s, 2065s ($^{13}\text{C}\equiv\text{N}$). δ_{C} (100.6 MHz, CD_2Cl_2 , 293 K): 144.85 (1C, d, $J_{\text{C-C}} = 7.3$, $^{13}\text{CN}_{\text{trans-C}}$), 131.55 (1C, d, $J_{\text{C-C}} = 7.3$, $^{13}\text{CN}_{\text{trans-N}}$).

Synthesis of $(\text{NBu}_4)[\text{Pd}(\text{ppy})(\text{CN})_2]$ (2**).** Compound **2** was synthesized in a similar way to **1**: KCN (318.0 mg, 4.883 mmol), $[\text{Pd}(\text{ppy})(\text{NCMe})_2]\text{ClO}_4$ (1080.0 mg, 2.442 mmol), NBu_4ClO_4 (835 mg, 2.442 mmol), yielding **2**, white solid, 1061.2 mg, 78%. Found: C, 62.73; H, 7.74; N, 9.94. Calcd (%) for $\text{C}_{29}\text{H}_{44}\text{N}_4\text{Pd}$: C, 62.75; H, 7.99; N, 10.09. $\nu_{\text{max}}/\text{cm}^{-1}$ 2122s, 2113s ($\text{C}\equiv\text{N}$). δ_{H} (300 MHz, CD_3COCD_3 , 293 K): 9.21 (1H, ddd, $J_{2,3} = 5.4$, $J_{2,4} = 1.6$, $J_{2,5} = 0.7$, 2-H), 8.10 (1H, m, 9-H), 7.9–7.8 (2H, m, 4-H, 5-H), 7.61 (1H, m, 6-H), 7.29 (1H, ddd, $J_{3,4} = 7.3$, $J_{3,2} = 5.4$, $J_{3,5} = 2.1$, 3-H), 6.97–7.05 (2H, m, 7-H, 8-H), 3.46 (8H, m, CH_2 , NBu_4^+), 1.82 (8H, m, CH_2 , NBu_4^+), 1.43 (8H, m, CH_2 , NBu_4^+), 0.96 (12H, t, $^3J_{\text{H-H}} = 7.3$, CH_3 , NBu_4^+). m/z (FAB $^-$) 312 ($[\text{Pd}(\text{ppy})(\text{CN})_2]^-$); Λ_{M} 37.05 $\Omega^{-1}\text{cm}^2\text{mol}^{-1}$, solution 5×10^{-4} M in methanol.

$(\text{NBu}_4)[\text{Pd}(\text{ppy})(^{13}\text{CN})_2]$ (**2'**) was prepared following the method described for **2**, but using K^{13}CN . $\nu_{\text{max}}/\text{cm}^{-1}$ 2076s, 2068s ($^{13}\text{C}\equiv\text{N}$). δ_{C} (100.6 MHz, CD_2Cl_2 , 293 K): 145.65 (1C, d, $J_{\text{C-C}} = 8.4$, $^{13}\text{CN}_{\text{trans-C}}$), 133.92 (1C, d, $J_{\text{C-C}} = 8.4$, $^{13}\text{CN}_{\text{trans-N}}$).

Synthesis of $[\text{PdTl}(\text{bzq})(\text{CN})_2]$ (3**).** A solution of the complex $(\text{NBu}_4)[\text{Pd}(\text{bzq})(\text{CN})_2]$ (422.8 mg, 0.73 mmol) in methanol (20 mL) is treated with TlPF_6 (245.0 mg, 0.701 mmol). After stirring at rt for 2 h, the resulting suspension was evaporated to dryness. Addition of CH_2Cl_2 (20 mL) to the residue rendered a pale yellow solid, which was filtered off and dried to give **3** (0.3314 g, 87%). Found: C, 33.07; H, 1.45; N, 7.71. Calcd for $\text{C}_{15}\text{H}_9\text{N}_3\text{PdTl}$: C, 33.29; H, 1.49; N, 7.76. $\nu_{\text{max}}/\text{cm}^{-1}$ 2132s, 2112s ($\text{C}\equiv\text{N}$); δ_{H} (400 MHz, CD_3OD , 293 K): 9.21 (1H, dd, $J_{2,3} = 5.6$, $J_{2,4} = 1.2$, 2-H), 8.47 (1H, dd, $J_{4,3} = 8.2$, $J_{4,2} = 1.2$, 4-H), 8.05 (1H, dd, $J_{9,8} = 7.0$, $J_{9,7} = 0.6$, 9-H), 7.80 (1H, d, $J_{5,6} = 8.8$, 5-H), 7.66 (1H, d, $J_{5,6} = 8.8$, 6-H), 7.62 (1H, dd, $J_{3,4} = 8.2$, $J_{3,2} = 5.6$, 3-H), 7.61 (1H, dd, $J_{7,8} = 7.6$, $J_{7,9} = 0.6$, 7-H), 7.46 (1H, dd, $J_{8,7} = 7.8$, $J_{8,9} = 7.0$, 8-H); m/z (FAB $^-$) 336 ($[\text{Pd}(\text{bzq})(\text{C}\equiv\text{N})_2]^-$, 100%); Λ_{M} 49.74 $\Omega^{-1}\text{cm}^2\text{mol}^{-1}$, solution 5×10^{-4} M in methanol.

Chart 1



Synthesis of $[\text{PdTi}(\text{ppy})(\text{CN})_2]$ (**4**) was performed following the method described for **3** with $(\text{NBu}_4)[\text{Pd}(\text{ppy})(\text{CN})_2]$ (200.0 mg, 0.387 mmol) and TIPF_6 (119.0 mg, 0.341 mmol), yielding **4**, pale yellow solid, 153.1 mg, 87%. Found: C, 30.06; H, 1.61; N, 8.15. Calcd for $\text{C}_{13}\text{H}_8\text{N}_3\text{PdTi}$: C, 30.20; H, 1.56; N, 8.12. $\nu_{\text{max}}/\text{cm}^{-1}$ 2118s, 2107s ($\text{C}\equiv\text{N}$). δ_{H} (400 MHz, CD_3OD , 293 K): 8.97 (1H, d, $J_{2,3} = 5.6$, 2-H), 7.85–7.97 (3H, m, 4-H, 5-H, 9-H), 7.62 (1H, m, 6-H), 7.26 (1H, ddd, $J_{3,4} = 7.6$, $J_{3,2} = 5.6$, $J_{3,5} = 1.6$, 3-H), 7.05–7.10 (2H, m, 7-H, 8-H). m/z (FAB⁻) 312 ($[\text{Pd}(\text{ppy})(\text{C}\equiv\text{N})_2]^-$, 100%). Λ_{M} 52.40 $\Omega^{-1} \text{cm}^2 \text{mol}^{-1}$, solution 5×10^{-4} M in methanol.

X-ray Structure Determinations. Single crystals of **3** and **4** were obtained by slow diffusion of methanol into a saturated dichloromethane solution. The crystal data, data collection parameters, and structure solution and refinement details for the crystal structures determined are summarized in Table S1, Supporting Information. Crystals were mounted at the end of quartz fibres. The radiation used in all cases was graphite monochromated Mo $K\alpha$ ($\lambda = 0.71073$ Å). X-ray intensity data were collected on an Oxford Diffraction Xcalibur diffractometer. The diffraction frames were integrated and corrected from absorption by using the CrysAlis RED program.⁷⁶

The structures were solved by Patterson and Fourier methods and refined by full-matrix least-squares on F^2 with SHELXL-97.⁷⁷ All non-hydrogen atoms were assigned anisotropic displacement parameters and refined without positional constraints. All hydrogen atoms were constrained to idealized geometries and assigned isotropic displacement parameters equal to 1.2 times the U_{iso} values of their attached parent atoms. Full-matrix least-squares refinement of these models against F^2 converged to final residual indices given in Table S1, Supporting Information.

■ ASSOCIATED CONTENT

■ Supporting Information

UV–vis absorption spectra of **1** and **2**, normalized diffused reflectance UV–vis spectra of **1–4** in the solid state, excitation and emission spectra of **1** and **2** at 77 K, excitation and emission spectra of **3** and **4** in solution of MeOH (10^{-3} M), emission spectra of **2** and **4** in solid state at 77 K, excitation and emission spectra of **3** and **4** at 77 K, X-ray structure analysis of **3** and **4**, and crystallographic data in CIF format. This material is available free of charge via the Internet at <http://pubs.acs.org>.

■ AUTHOR INFORMATION

■ Corresponding Author

*E-mail: sicilia@unizar.es.

■ Notes

The authors declare no competing financial interest.

■ ACKNOWLEDGMENTS

This work was supported by the Spanish MICINN/FEDER (Project CTQ2008-06669-C02) and the Gobierno de Aragón (Grupo Consolidado, Química Inorgánica y de los Compuestos Organometálicos).

■ REFERENCES

- Pignolet, L. H.; Aubart, M. A.; Craighead, K. L.; Gould, R. A. T.; Krogstad, D. A.; Wiley, J. S. *Coord. Chem. Rev.* **1995**, *143*, 219–263.
- Pyykko, P. *Chem. Rev.* **1997**, *97*, 597–636.
- Pyykko, P. *Angew. Chem., Int. Ed.* **2004**, *43*, 4412–4456.
- Doerrer, L. H. *Comments Inorg. Chem.* **2008**, *29*, 93–127.
- Sivaramakrishna, A.; Clayton, H. S.; Makhubela, B. C. E.; Moss, J. R. *Coord. Chem. Rev.* **2008**, *252*, 1460–1485.
- Qiu, S.; Zhu, G. *Coord. Chem. Rev.* **2009**, *253*, 2891–2911.
- Sculfort, S.; Braunstein, P. *Chem. Soc. Rev.* **2011**, *40*, 2741–2760.
- Aullon, G.; Alvarez, S. *Inorg. Chem.* **1996**, *35*, 3137–3144.
- Mealli, C.; Pichierri, F.; Randaccio, L.; Zangrando, E.; Krumm, M.; Holtenrich, D.; Lippert, B. *Inorg. Chem.* **1995**, *34*, 3418–3424.

(10) Forniés, J.; Martin, A. In *Metal Clusters in Chemistry*; Braunstein, P., Oro, L. A., Raithby, P. R., Eds.; Wiley-VCH Verlag GmbH: Weinheim, Germany, 1999; Vol. 1, pp 417–443.

(11) Ara, I.; Falvello, L. R.; Forniés, J.; Gómez-Cordon, J.; Lalinde, E.; Merino, R. I.; Uson, I. J. *Organomet. Chem.* **2002**, *663*, 284–288.

(12) Berenguer, J. R.; Lalinde, E.; Moreno, M. T. *Coord. Chem. Rev.* **2010**, *254*, 832–875.

(13) Berenguer, J. R.; Fernández, J.; Gil, B.; Lalinde, E.; Sánchez, S. *Inorg. Chem.* **2010**, *49*, 4232–4244.

(14) Gil, B.; Forniés, J.; Gómez, J.; Lalinde, E.; Martín, A.; Moreno, M. T. *Inorg. Chem.* **2006**, *45*, 7788–7798.

(15) Yin, G.-Q.; Wei, Q.-H.; Zhang, L.-Y.; Chen, Z.-N. *Organometallics* **2006**, *25*, 580–587.

(16) Lang, H.; del Villar, A.; Stein, T.; Zoufala, P.; Rueffer, T.; Rheinwald, G. *J. Organomet. Chem.* **2007**, *692*, 5203–5210.

(17) Ara, I.; Berenguer, J. R.; Forniés, J.; Gomez, J.; Lalinde, E.; Merino, R. I. *Inorg. Chem.* **1997**, *36*, 6461–6464.

(18) Charmant, J. P. H.; Forniés, J.; Gómez, J.; Lalinde, E.; Merino, R. I.; Moreno, M. T.; Orpen, A. G. *Organometallics* **2003**, *22*, 652–656.

(19) Berenguer, R. J.; Díez, A.; Fernández, J.; Forniés, J.; García, A.; Gil, B.; Lalinde, E.; Moreno, M. T. *Inorg. Chem.* **2008**, *47*, 7703–7716.

(20) Berenguer, J. R.; Gil, B.; Fernández, J.; Forniés, J.; Lalinde, E. *Inorg. Chem.* **2009**, *48*, 5250–5262.

(21) Forniés, J.; Ibañez, S.; Martín, A.; Sanz, M.; Berenguer, J. R.; Lalinde, E.; Torroba, J. *Organometallics* **2006**, *25*, 4331–4340.

(22) Falvello, L. R.; Forniés, J.; Lalinde, E.; Menjón, B.; García-Monforte, M. A.; Moreno, M. T.; Tomas, M. *Chem. Commun.* **2007**, 3838–3840.

(23) Forniés, J.; Sicilia, V.; Casas, J. M.; Martín, A.; López, J. A.; Larraz, C.; Borja, P.; Ovejero, C. *Dalton Trans.* **2011**, *40*, 2898–2912.

(24) Pyykko, P.; Desclaux, J. P. *Acc. Chem. Res.* **1979**, *12*, 276–281.

(25) Forniés, J.; Fuertes, S.; Martín, A.; Sicilia, V.; Gil, B.; Lalinde, E. *Dalton Trans.* **2009**, 2224–2234 and references therein.

(26) Forniés, J.; Ibañez, S.; Martín, A.; Gil, B.; Lalinde, E.; Moreno, M. T. *Organometallics* **2004**, *23*, 3963–3975.

(27) Jamali, S.; Mazloomi, Z.; Nabavizadeh, S. M.; Milic, D.; Kia, R.; Rashidi, M. *Inorg. Chem.* **2010**, *49*, 2721–2726.

(28) Janzen, D. E.; Mehne, L. F.; VanDerveer, D. G.; Grant, G. J. *Inorg. Chem.* **2005**, *44*, 8182–8184.

(29) Fuertes, S.; Woodall, C. H.; Raithby, P. R.; Sicilia, V. *Organometallics* **2012**, *31*, 4228–4240.

(30) Yamaguchi, T.; Yamaguchizaki, F.; Ito, T. *J. Am. Chem. Soc.* **2001**, *123*, 743–744.

(31) Yamaguchi, T.; Yamazaki, F.; Ito, T. *J. Am. Chem. Soc.* **1999**, *121*, 7405–7406.

(32) Oberbeckmann-Winter, N.; Morise, X.; Braunstein, P.; Welter, R. *Inorg. Chem.* **2005**, *44*, 1391–1403.

(33) Díez, A.; Lalinde, E.; Teresa Moreno, M. *Coord. Chem. Rev.* **2011**, *255*, 2426–2447.

(34) Wong, K. M. C.; Hui, C. K.; Yu, K. L.; Yam, V. W. W. *Coord. Chem. Rev.* **2002**, *229*, 123–132.

(35) Chen, Z.-N.; Zhao, N.; Fan, Y.; Ni, J. *Coord. Chem. Rev.* **2009**, *253*, 1–20.

(36) Forniés, J.; García, A.; Lalinde, E.; Moreno, M. T. *Inorg. Chem.* **2008**, *47*, 3651.

(37) Elbjerrami, O.; Rawashdeh-Omary, M. A.; Omary, M. A. Res. *Chem. Intermed.* **2011**, *37*, 691–703.

(38) Forniés, J.; Ibañez, S.; Lalinde, E.; Martín, A.; Moreno, M. T.; Tsiapis, A. C. *Dalton Trans.* **2012**, *41*, 3439–3451.

(39) Falvello, L. R.; Forniés, J.; Martín, A.; Sicilia, V.; Villarroja, P. *Organometallics* **2002**, *21*, 4604–4610.

(40) Forniés, J.; Navarro, R.; Tomás, M.; Urriolabeitia, E. P. *Organometallics* **1993**, *12*, 940–943.

(41) Ponec, R.; Bučinský, L. S.; Gatti, C. J. *Chem. Theory Comput.* **2010**, *6*, 3113–3121.

(42) Pyykkö, P. *Chem. Rev.* **1988**, *88*, 563.

(43) Pitzer, K. S. *Acc. Chem. Res.* **1979**, *12*, 271–276.

- (44) Reitsamer, C.; Schuh, W.; Kopacka, H.; Wurst, K.; Peringer, P. *Organometallics* **2009**, *28*, 6617–6620.
- (45) Liu, I. P.-C.; Chen, C.-H.; Chen, C.-F.; Lee, G.-H.; Peng, S.-M. *Chem. Commun.* **2009**, 577–579.
- (46) Sharma, S.; Baligar, R. S.; Singh, H. B.; Butcher, R. J. *Angew. Chem., Int. Ed.* **2009**, *48*, 1987–1990.
- (47) Alonso, E.; Forniés, J.; Fortuño, C.; Lledós, A.; Martín, A.; Nova, A. *Inorg. Chem.* **2009**, *48*, 7679–7690.
- (48) Lanci, M. P.; Remy, M. S.; Kaminsky, W.; Mayer, J. M.; Sanford, M. S. *J. Am. Chem. Soc.* **2009**, *131*, 15618–15620.
- (49) Vicente, J.; Gonzalez-Herrero, P.; Perez-Cadenas, M.; Jones, P. G.; Bautista, D. *Inorg. Chem.* **2007**, *46*, 4718–4732.
- (50) Heckenroth, M.; Neels, A.; Garnier, M. G.; Aebi, P.; Ehlers, A. W.; Albrecht, M. *Chem.—Eur. J.* **2009**, *15*, 9375–9386.
- (51) Kim, M.; Taylor, T. J.; Gabbai, F. P. *J. Am. Chem. Soc.* **2008**, *130*, 6332–6333.
- (52) Maliarik, M.; Nagle, J. K.; Ilyukhin, A.; Murashova, E.; Mink, J.; Skripkin, M.; Glaser, J.; Kovacs, M.; Horvath, A. *Inorg. Chem.* **2007**, *46*, 4642–4653.
- (53) Alonso, E.; Forniés, J.; Fortuño, C.; Martín, A.; Orpen, A. G. *Organometallics* **2003**, *22*, 5011–5019.
- (54) Bronger, W.; Bonsmann, B. Z. *Anorg. Allg. Chem.* **1995**, *621*, 2083.
- (55) Balch, A. L.; Davis, B. J.; Fung, E. Y.; Olmstead, M. M. *Inorg. Chim. Acta* **1993**, *212*, 149–156.
- (56) Klepp, K. O. *J. Less-Common Met.* **1985**, *107*, 147.
- (57) Forniés, J.; Fuertes, S.; Lopéz, J. A.; Martín, A.; Sicilia, V. *Inorg. Chem.* **2008**, *47*, 7166–7176.
- (58) Dunbar, K. R.; Heintz, R. A. *Prog. Inorg. Chem.* **1997**, *45*, 283.
- (59) Forniés, J.; Fuertes, S.; Larraz, C.; Martín, A.; Sicilia, V.; Tsipis, A. C. *Organometallics* **2012**, *31*, 2729–2740.
- (60) Kaltsoyannis, N. J. *J. Chem. Soc., Dalton Trans.* **1996**, 1.
- (61) Fairlamb, I. J. S.; Kapdi, A. R.; Lee, A. F.; Sánchez, G.; López, G.; Serrano, J. L.; García, L.; Pérez, J.; Pérez, E. *Dalton Trans.* **2004**, 3970.
- (62) Sánchez, G.; García, J.; Meseguer, D.; Serrano, J. L.; García, L.; Pérez, J.; López, G. *Dalton Trans.* **2003**, 4709.
- (63) Yip, H. K.; Lai, T. F.; Che, C. M. *J. Chem. Soc., Dalton Trans.* **1991**, 1639.
- (64) Oberhauser, W.; Bachmann, C.; Stampfl, T.; Haid, R.; Langes, C.; Rieder, A.; Brüggeller, P. *Polyhedron* **1998**, *17*, 3211.
- (65) Ng, S. W.; Zuckerman, J. J. *Adv. Inorg. Chem. Radiochem.* **1985**, *29*, 297.
- (66) Stork, J. R.; Olmstead, M. M.; Balch, A. L. *J. Am. Chem. Soc.* **2005**, *127*, 6512.
- (67) Stork, J. R.; Olmstead, M. M.; Fettingner, J. C.; Balch, A. L. *Inorg. Chem.* **2006**, *45*, 849.
- (68) Nagle, J. K.; Balch, A. L.; Olmstead, M. M. *J. Am. Chem. Soc.* **1988**, *110*, 319.
- (69) Zank, J.; Schier, A.; Schmidbaur, H. *J. Chem. Soc., Dalton Trans.* **1999**, 415–420.
- (70) Bayler, A.; Schier, A.; Bowmaker, G. A.; Schmidbaur, H. *J. Am. Chem. Soc.* **1996**, *118*, 7006–7007.
- (71) Tripathi, U. M.; Bauer, A.; Schmidbaur, H. *J. Chem. Soc., Dalton Trans.* **1997**, 2865–2868.
- (72) Cocker, T. M.; Bachman, R. E. *Inorg. Chem.* **2001**, *40*, 1550–1556.
- (73) DePriest, J.; Zheng, G. Y.; Goswami, N.; Eichhorn, D. M.; Woods, C.; Rillema, D. P. *Inorg. Chem.* **2000**, *39*, 1955.
- (74) Neve, F.; Crispini, A.; Di Pietro, C.; Campagna, S. *Organometallics* **2002**, *21*, 3511–3518.
- (75) Díez, A.; Forniés, J.; Fuertes, S.; Lalinde, E.; Larraz, C.; Lopéz, J. A.; Martín, A.; Moreno, M. T.; Sicilia, V. *Organometallics* **2009**, *28*, 1705–1718.
- (76) *CrysAlis RED Program for X-ray CCD camera data reduction*; Oxford Diffraction Ltd: Oxford, UK, 2005–2006.
- (77) Sheldrick, G. M., *SHELXL-97 Program for crystal structure refinement from diffraction data*; University of Göttingen: Göttingen, Germany, 1997.